Proceedings of IMECE2006
2006 ASME International Mechanical Engineering Congress and Exposition
November 5-10, 2006, Chicago, Illinois, USA

IMECE2006-15902

NONLINEAR MODELING AND EXPERIMENTAL VALIDATION OF TIRE NONUNIFORMITY INDUCED TANGENTIAL STEERING WHEEL VIBRATIONS

Virgile Ayglon
Smart Structure and NEMS Laboratory, Department of Mechanical Engineering, Clemson University, Clemson, SC 29634

Nader Jalili *
Smart Structure and NEMS Laboratory, Department of Mechanical Engineering, Clemson University, Clemson, SC 29634

Imtiaz Haque
Department of Mechanical Engineering, Clemson University, Clemson, SC 29634

ABSTRACT

This paper describes the model integration and validation that followed the development of nonlinear models of a tire with non-uniformities, a double wishbone suspension and rack-and-pinion power steering. These submodels are integrated to investigate the effects of variation of tire, suspension and steering parameters on the transmission of tire forces acting on the wheel spindle to the steering system and vehicle chassis. The tire model is based on a rigid ring model which includes mass imbalance and balancing mass. The suspension is idealized as rigid links with seven degrees-of-freedom and the bushings are represented by spring-damper elements. The equations of motion are derived using the Lagrange multiplier method in Maple, and solved numerically using Matlab DAE solver. The steering system is idealized as a four degree-of-freedom system and considers motion of the rack, rack housing, pinion gear and steering wheel. Nonlinear compliant friction is considered between the pinion gear / rack, and the steering column / chassis interfaces. The analytical model is used to develop a quantitative measure of the relative importance of the parameters such as mass/inertia, suspension bushing stiffness and damping, torsion bar stiffness and damping, rack friction and damping, to the force transmissibility to the vehicle chassis and the steering system. Experimental results include a modal analysis, a shop-testing and road testing, which are used to cross verify the numerical simulations. The testing shows the variation of forces in the steering system due to tire imbalances, emphasizing the nonlinear variation of the nibble phenomenon with vehicle speed and tire imbalance. Results obtained from simulation matches well with the experimental measurements.

INTRODUCTION

The perceived level of vehicle comfort of driver and passengers can be severely reduced due to unwanted noise, vibrations or harshness. While these factors can be measured objectively, human responses may vary from one individual to another. In an effort to relate these levels of discomfort to human perception, subjective assessments are often used by tire and vehicle manufacturers to develop sensitivity thresholds or evaluate their designs. Such discomforts can result from external factors such as road surface irregularities and aerodynamic forces, or internal sources such as engine and transmission vibrations, suspension and chassis dynamics, or harmonic excitations resulting from tire non-uniformities; the last one of which can cause excessive torsional steering wheel vibrations known as “steering nibble”.

The primary objectives of this research are to characterize the transmission of these vibrations through the validation of an integrated simulation model and develop an objective assessment of the steering nibble vibrations correlated against subjective nibble ratings. Thus, it forms a basis of the understanding of the system variables that affect the vibration, force and torque transmission from the wheel spindle to the steering wheel, and how variation in these system parameters affect the vibration transmission in general. The models described herein are made general enough to simulate the effects of system parameter variation, for any vehicle with a similar configuration, i.e., a double wishbone front suspension with a power assisted rack-and-pinion steering.

SYSTEM OVERVIEW AND MODELING APPROACH

The development of the subsystem followed a modular approach so that each submodel can be modified independently without affecting other subsystems. Based on the research conducted by Cherian *et al*. [4], a steering and suspension models representative of the test vehicle have been developed. In parallel, Dillinger *et al*. [7] and Mangun *et al*. [11] have developed non-uniform tire models.

* Assistant Professor and author of correspondence, Email: jalili@clemson.edu.

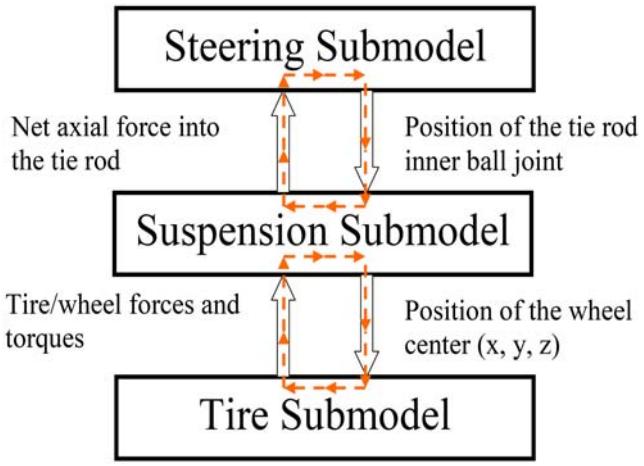

Figure 1. Model integration approach

The model integration approach is shown in Figure 1. At each time step, the initial conditions (IC) of the tire model are calculated; the tire model passes the corresponding torque and forces acting at the hub to the suspension; the suspension's IC and constrained forces are computed; the suspension response is simulated and passes the net axial force in the tie rod based on the deflection in the tie rod; the steering response is then simulated based on the input tie rod forces and the position of the inner ball joint is updated based on the motion of the steering rack for calculating the deflection in the tie rod for the next iteration; the position of the wheel center based on the suspension motion is also updated to calculate the tire forces for
the next iteration.

Steering Subsystem Model:

Bosworth [3] conducted a design of experiment (DOE) study on a rack-and-pinion with McPherson strut front suspension to optimize for eight parameters found to be most influential on steering nibble. A brainstorming yielded 250 candidate parameters which were then reduced to 8 by control criteria and classification. A detailed finite element model of the steering wheel response to mass imbalance was developed using NASTRAN® and was validated with experimental data. The four major parameters affecting the optimization were the steering rack damping, the rack mount bushing lateral rate, Lower Control Arm bushing fore-aft rate, and tie rod bushing fore-aft and radial rate. Following the optimization, the steering wheel vibrations were reduced by 40 %.

Kim *et al.* [8] (1996) analyzed a chassis system to reduce steering shimmy and brake judder vibrations. These two phenomena are considered simultaneously due to the similar nature of their transfer paths and exciting source. They are perceived as torsional steering wheel vibrations and vehicle body lateral vibration. Steering shimmy is mostly influenced by tire/wheel imbalance, hub bearing run-out and suspension bushing compliance resulting in force variation at the wheel hub. The brake judder is excited by the fore-aft vibrations due to the brake rotor thickness variation (RTV). Sensitivity to fore-aft forces would also entail sensitivity to tire non-uniformity as it is also known to produce strong fore-aft force variations.

Pak *et al.* [15] investigated the effects of tire non-uniformity of the steering wheel vibrations. The analysis considered both shake and shimmy due to tire non-uniformity. The simulation model includes a 19 DOF steering system, with inclusion of structural viscous damping and dry friction. The vehicle body is modeled with 4 DOF consisting of 1st and 2nd lateral bending and 1st torsional and vertical bending mode. In addition, the transmission and engine mount are modeled with 6 DOF. Finally, the tire is considered as the source of excitation and includes mass imbalance, stiffness non-uniformity as well as radial and lateral run-out. Hamilton principle was used to derive the subsequent equation of motion of the whole system. Principles of vibrations were then used to determine the response under free vibration and forced vibration. Results were then compared with experimental data. Radial force variation (RFV) and longitudinal force variation (LFV) were found to be velocity independent. Tangential force variation (TFV), however, was largely proportional to the angular velocity square and a function of run-out. TFV had the most effect on the amplitude of the shimmy. Good prediction of the steering shimmy could be made using the simulation model. As reported by Neureder [13, 14], the frictional characteristic present in this steering system was found to be rather compliant, contrary to the Coulomb and dry friction assumption generally found in most publications. Thus, Neureder (2001, 2002) considered a non-coulomb friction model wherein the force does not need to exceed the minimum value of static friction before it transmits a motion to pinion.

The model used by Neureder (2001, 2002) forms the basis of the model considered in this study. The schematic of the steering subsystem model is shown in Figure 2. The steering wheel is modeled using the lumped inertia I_{SW} and the angular position of the hand wheel is defined as θ_{SW}. The torsional bushing is approximated by the static stiffness and damping rate K_b and C_b, respectively. The steering column is similarly modeled as a spring-damper element which represents the equivalent stiffness and damping properties resulting from the coupling of the steering column and the torsion bar. The steering column is then connected to the pinion. The pinion gear motion θ_p depends solely on the motion of the rack as an ideal mesh between the pinion gear and rack gear is assumed. The rack is given the ability to move in the axial x-direction. The mass of the rack is given by the lumped parameter M_r. The hydraulic viscous damping present in the rack housing is modeled by the damping coefficient C_d. The internal friction between the rack and housing is modeled as compliant by a spring in series with a stick/slip element. This aspect of the modeling had been discussed by Neureder, and it was also mentioned in other publications [14, 18]. The power steering is modeled by a static power boost rate based on the wind up in

the torsion bar. This is an acceptable approximation for small steering angle of less than 1 degree as found from experimental testing. The power boost force affects both the motion of the rack and housing. The rack housing is allowed to move along the y-direction. It is firmly mounted to the vehicle chassis by means of rubber bushings modeled by the spring-damper elements K_h and C_h, respectively. The steering model includes three DOF; namely the steering wheel angular displacement, the rack lateral motion and the housing axial displacement. Due to the ideal mesh assumption between the pinion and rack gear, the pinion gear is not allowed any DOF. The equations representing the steering subsystem dynamics can be given as:

$$M_r\ddot{x} = F_{tr} - f_r - B(\theta_{sw} - \theta_p) - C_d(\dot{x} - \dot{y}) - F_p \quad (1)$$

$$M_h\ddot{y} = f_r + B(\theta_{sw} - \theta_p) + C_d(\dot{x} - \dot{y}) - K_h y - C_h\dot{y} \quad (2)$$

$$I_p\ddot{\theta}_p = K_{sc}(\theta_{sw} - \theta_p) + C_{sc}(\dot{\theta}_{sw} - \dot{\theta}_p) + F_p r_p \quad (3)$$

$$I_{sw}\ddot{\theta}_{sw} = K_{sc}(\theta_p - \theta_{sw}) + C_{sc}(\dot{\theta}_p - \dot{\theta}_{sw}) - K_b\theta_{sw} - C_b\dot{\theta}_{sw} - f_{sc} \quad (4)$$

where the parameters are defined in Appendix A, and the displacements x, y, θ_{sw} and θ_p represent the displacement of the rack, housing, steering wheel and pinion, respectively, and their derivatives represent the velocity and acceleration of the parts.

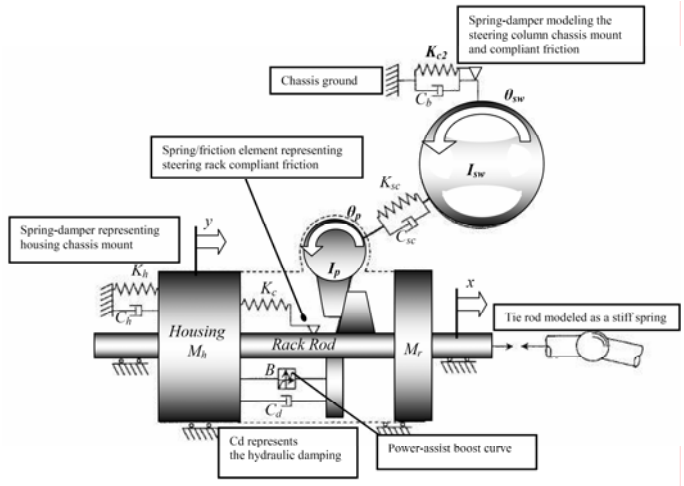

Figure 2. Schematic of the steering subsystem model.

For numerical simulations, some of the parameters for this model were extracted from the model provided by Michelin, while others were estimated by varying the parameters in the numerical simulation to match the results from experiment.

Tire Subsystem Model:

Mancosu *et al.* [10] have described a planar rigid ring tire model for the study of vehicle ride comfort. The results obtained from the developed model are validated by comparison to a finite element model and performing an eigenvalue analysis. The tire vibrations are found to be essentially composed of rigid body modes in the frequency range of 0 to 130 Hz. The model is able to match the experimental results quite closely in that frequency range.

Stutts *et al.* [17] elaborated a tire model that included concentrated radial stiffness non-uniformity. A rigid tread ring supported by a viscoelastic foundation is used to model the tire. The radial stiffness was found to affect the force variation in the tire, most notably the fore-aft force variation. It was shown that the concentrated stiffness non-uniformity influences the fore-aft force at twice the rotational frequency of the wheel, thus contributing to second harmonic force variations. Furthermore, the parametric resonance of maximum amplitude occurs at a vehicle speed corresponding to half of the tire natural frequency.

Dillinger *et al.* [7] have developed non-uniform tire models based on Stutts *et al.* modeling to include the effects of tire stiffness non-uniformity, mass imbalance and balancing, radial run-out, longitudinal slip, and sidewall hysteresis. Upon completion of the model development, a comparison of the effects of the aforementioned parameters is given. Simulated tangential and radial force variations are validated with experimental results measured on a High Speed Uniformity (HSU) machine. These models considered only planar tire dynamics. Mangun *et al.* [11] undertook the improvement of these models to include additional DOF in order to simulate the tire motion as it occurs for on-road conditions in three dimensional space.

The mathematical formulation of the tire model conducted by Mangun *et al.* [11] is based on previous work conducted by Dillinger *et al.* [7]. It is briefly presented here as it is the main component of force and torque variations acting on the suspension hub. The first model is based on a rigid ring model attached to a fixed hub via a series of distributed springs and damper elements, and subjected to a no-slip condition as shown in Figure 3.

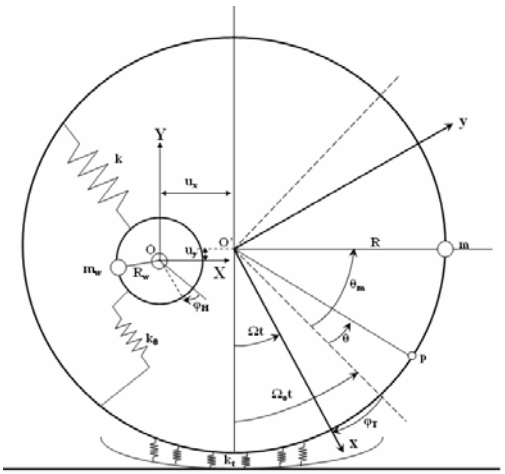

Figure 3. Planar tire model schematic

The second model is identical to the first model with the exception that the hub is now considered to be moving with a constant velocity in the x-direction only. The third model made

a more drastic step toward the improvement of the model kinematics by considering motion in three dimensional space. Camber and steer DOF were added to the model as well as the effects of a counter balancing mass as shown in Figure 4.

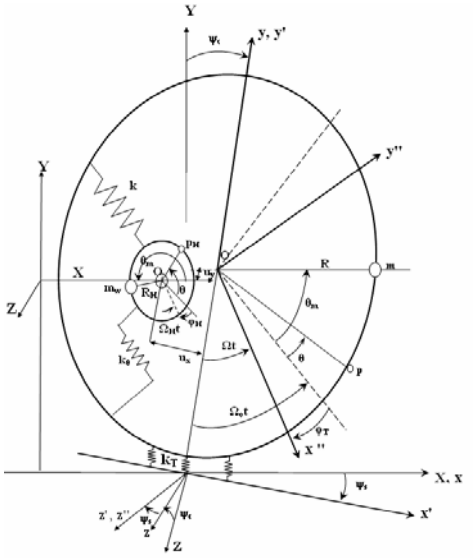

Figure 4. Rigid ring tire model with camber and steer

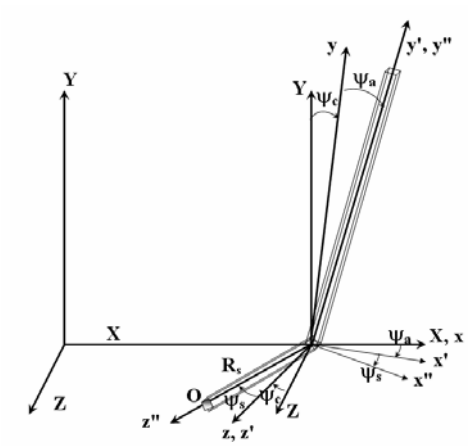

Figure 5. Moment arm schematic

The fourth model builds on the previous model to include the effects of a moment arm as shown in Figure 5. This last step was of critical importance since, the offset of the tire/wheel assembly produces aligning moments that act on the principle axes of the suspension.

A Lagrangian approach was chosen for the mathematical formulation of the model and followed the following procedure outlined by Mangun *et al.* [11]. The Lagrangian is expressed as the difference between the kinetic and potential energies; $L = T - V$. Adding the dissipated energy (R), Lagrange's equation is used to derive the EOM:

$$\frac{d}{dt}\left(\frac{\partial L}{\partial \dot{q}_i}\right) - \left(\frac{\partial L}{\partial q_i}\right) + \left(\frac{\partial R}{\partial \dot{q}_i}\right) = Q_i \quad i = 1,\ 2, ..., n \tag{5}$$

Using the procedure outlined above, the equation of motion are derived in matrix form:

$$M\ddot{q} + C\dot{q} + Kq = Q\ , \qquad q = \begin{Bmatrix} \phi_H \\ \phi_T \\ u_y \end{Bmatrix} \tag{6}$$

Table 1: Tire parameter values used for the modeling of the non-uniform tire

Tire parameters	Symbols	Values
Effective rolling radius	R	381.9 mm
Balancing mass radius from wheel center	R_H	228.6 mm
Mass moment of inertia of the hub	I_H	0.4741 kg-m2
Mass of the wheel	m_H	9.073 kg
Mass of tread ring	m_T	6.96 kg
Contact patch vertical stiffness	K_{tz}	108593.2 N/m
Contact patch vertical damping coefficient	C_{tz}	624.85 N-s/m
Cornering stiffness	k_α	25486 N/rad

SIMULATION RESULTS AND DISCUSSIONS

Following the virtual Kinematics and Compliance (K & C) test presented in IMECE2005-81581, the submodels are integrated to complete the dynamic analysis.

Integrated Model Simulation Results:

Using experimental data obtained from the testing procedures, the simulation model can be validated though comparison of the results. The key components of this comparison are the tie rod forces (model's input) and the steering wheel angular acceleration (model's output). Since the vibrations felt by the driver at the steering wheel are used for the nibble rating, it was essential to accurately predict the steering wheel response both in time-domain and frequency-domain at any given vehicle speed. Hence, time history and PSDs were used for the comparison. Plots comparing the steering wheel angular acceleration for an imposed 30 g imbalance at four vehicle speeds within the critical range (65, 70, 75 and 80 mph) are given in Figures 6.

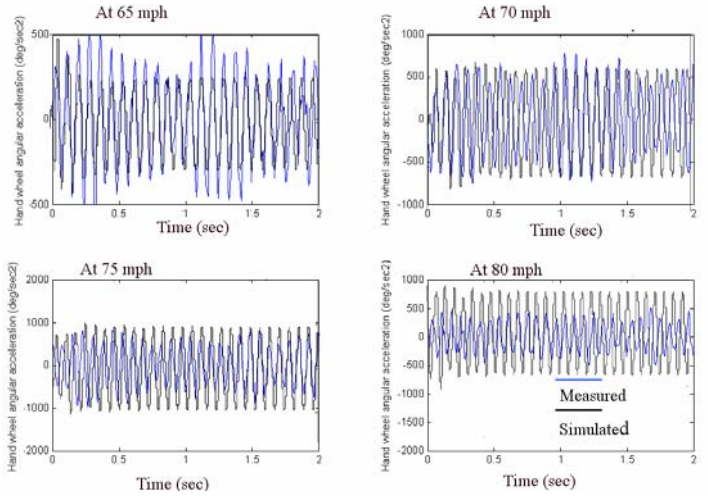

Figure 6. Measured and simulated steering wheel angular acceleration

The results from the figure above compare favorably. The characteristic resonance of 13.8 Hz occurring at 75 mph is also validated. However, the simulated steering wheel responses are higher than measured. From conducting the modal analysis, it was found that the response of the steering wheel at the resonance frequency can be more than seven times higher than average. The alignment of the resonant and driving frequencies thus plays a critical role in reproducing the resonance phenomenon. This explains why the simulated magnitudes may be higher. Also, the steering model has been developed to reproduce the nonlinear friction characteristics measured on the vehicle, though without consideration of energy dissipation components such as ball-joint friction. This idealization contributes to the lack of energy dissipation present in the physical system and thus the steering wheel accelerations are overestimated. Despite this discrepancy, reconcilable based on the model's limitations, the experimental results are well in agreement with the simulated results. Frequency responses were also investigated since the frequency content of the acceleration has an important effect on the human perception. PSDs of the steering wheel angular acceleration at the four vehicle speeds considered previously are given in Figure 7.

The PSDs of the steering wheel acceleration show similar frequency content. The simulated frequency responses are shifted about 5 to 8 dB higher than the experimental measurements. However, the trend, shapes and relative magnitudes of the PSDs are very close. As shown in the experimental testing, the peak resonance shifts with the driving frequency of the tire/wheel assembly as it produces a force variation at different frequencies corresponding to the rotational velocity of the wheel at that particular vehicle speed. This phenomenon is well reproduced by the model. The discrepancies in the PSDs are attributed to the same factors described previously.

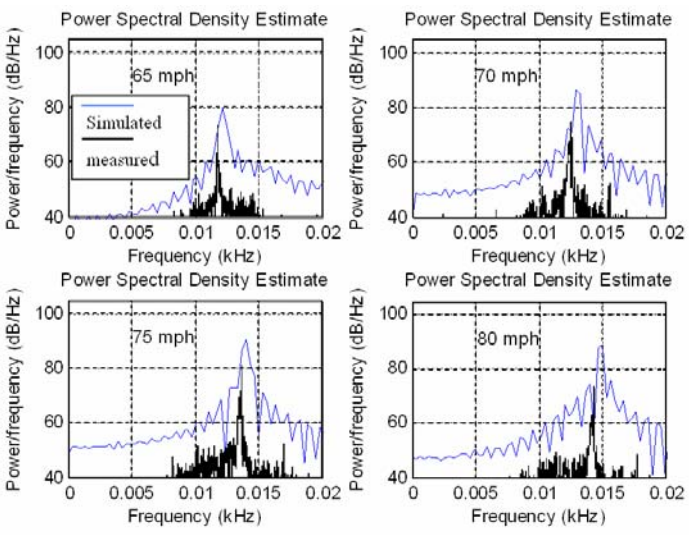

Figure 7. Measured and simulated steering wheel angular acceleration PSD

The final part of the model validation involved the comparison of the tie rod forces as shown in Figure 8. The tie rod force variations are not as well in agreement than the steering wheel response. The amplitude of the simulated tie rod forces are lower than experimentally measured.

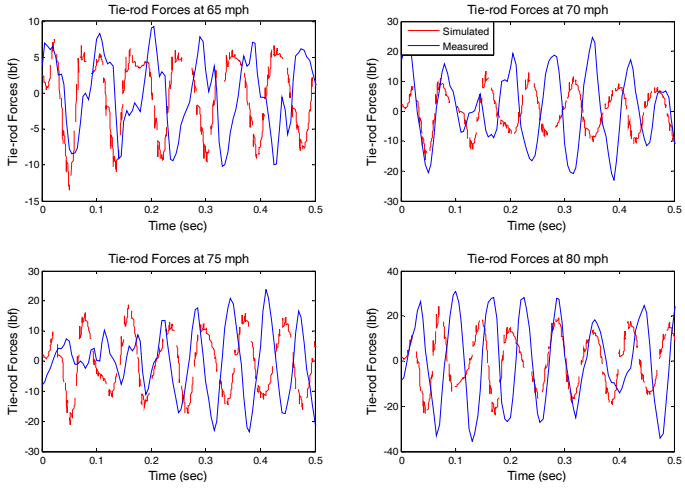

Figure 8. Measured and simulated tie rod force variation

Several factors are believed to be the cause of this discrepancy. The first factor is due to the fact that the tie rods were modeled as stiff linear springs. From the calibration testing of the strain gauge measuring the tie rod forces, it was found that this assumption is valid only for loads not exceeding certain values. Even though the tie rod stiffness was estimated based on its constituent material properties, the chosen stiffness is somewhat arbitrary. By adjusting the spring stiffness, the force amplitude would increase accordingly. Stiffening the tie rod contributed to reducing this discrepancy while generating

two undesirable outcomes; the steering wheel responses no longer represented the measured magnitudes as accurately as before, and the high stiffness introduced discontinuities and difficulties in the numerical solver.

The second factor is due to the assumption that the tie rod forces are directly transmitted in line with the motion of the rack. However, in the actual vehicle, the force may be transmitted at some angle, which would imply that only a fraction of the total force would be transmitted. Furthermore, the inclusion of lateral tire forces reduced the tie rod forces. The lateral tire forces are based on many idealizations and parameter estimations. The reason for including them in the model was to limit the rotation about the king-pin axis to better reproduce the measured steer angles.

The third factor is due to the inherent error in the experimental calibration of the strain gauges. The gain values for the strain gauges are obtained from the slopes of the load versus output voltage curves. Due to the nature of the tie rod, the gain value for converting the output voltage to its equivalent force is very large and not always linear. In other words, a small error in the output voltage would induce a very large change in the measured tie rod forces. In the light of all these factors and limiting assumptions made, the discrepancy in the tie rod forces is reasonably small.

Based on the results comparison, the model is considered validated. The discrepancies discussed previously are based on the fact that the simulation model is a simplified representation of a complex, highly nonlinear system in which each intermediate calculation may carry further numerical errors. It is important to recall that the main objective of this model is to predict the steering wheel nibble based on a given amount of tire non-uniformity. Intermediate steps are less significant. The prediction of steering nibble vibrations for a given imposed tire imbalance is deemed acceptable.

Experimental Results:

The steering friction is characterized by a nonlinear compliant stiffness that varies with the amplitude of excitation which produces an additional resonant frequency in the system. Figure 9 shows the resonance phenomenon as it occurs in the test vehicle. This figure was obtained from experimental measurements. Using the modal testing, a series of peak resonant frequencies of the steering wheel were extracted for few tests at different tie rod amplitude forces. These data points were then curve fitted using an exponential decaying function, since the exponential model yielded the best match and made reasonable physical sense. This curve fit is represented by the decreasing dotted line. From experimental testing at different speeds, tie rod forces were similarly recorded and the vehicle speed was converted to the rotational frequency of the wheel in Hertz. The tie rod force variation was plotted versus the rotational frequency of the wheel and a quadratic curve fit was obtained. The process was repeated for 3 different mass imbalance tests and the results were combined onto a single graph. As seen from Figure 9, the curves intersect at around 13.8 Hz which corresponds to the critical speed of 75 mph. This indicates that when the vehicle is within a 70 – 75 mph speed range, which corresponds to the resonance zone in Figure 9, the tie rod force variation is such that the resonant frequency is

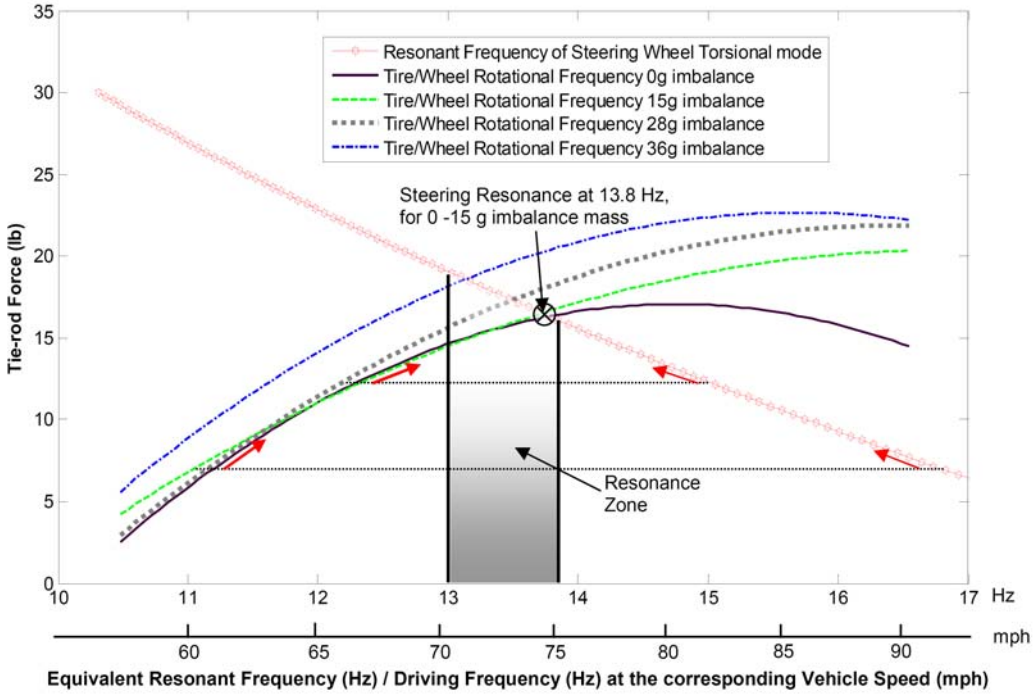

Figure 9. Steering resonance phenomenon

equal to the rotational frequency of the tire/wheel assembly, thus inducing an overall resonance in the steering system.

Subjective Testing Results:

Part of the subjective testing had to do with developing threshold of sensitivity to nibble vibrations. The threshold was found using least square fitting of a quadratic function using experimental data. The nibble rating data was fitted using the following form:

$$NibbleRating = a + b \times (Left\_mass)^2 + c \times (Right\_mass)^2 \quad (7)$$

Similarly to Equation (7), steering angular accelerations were fitted using only one quadratic term. The results from threshold development are presented in the following figures. Figure 10 shows the least square fitting of the nibble ratings versus the steering wheel angular acceleration.

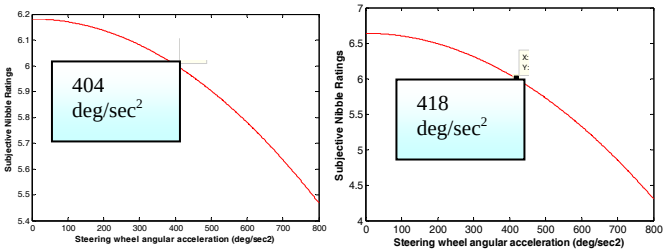

Figure 10. Subjective nibble rating vs. steering wheel angular acceleration for LPG track testing

In both cases, the threshold is consistently the same and both are very close to the threshold given in other references, around 400 deg/s^2.

The measured RMS value for the steering wheel acceleration and tie rod forces versus mass imbalance and speed is shown on Figures 11 and 12. The testing results predicted the measured thresholds of 400 deg/sec^2. For a speed of 75 mph or higher, and a mass imbalance of 28g or higher, the amplitude of the steering wheel vibrations are above the threshold value of 400 deg/sec^2.

CONCLUSIONS AND FUTURE WORK

The simulation model was developed and system parameters were tuned to represent the steering resonance phenomenon to a certain level of accuracy. A comparison of the simulation and experimental results led to the validation of the model for a range of vehicle speed and mass imbalance non-uniformity. Using the simulation model, the steering wheel angular acceleration could be predicted for a given imbalance weight and vehicle speed. The first harmonic of the forces produced due to the tire imbalance, particularly the tangential force variation (TFV), are the fundamental source of force variation exciting the nibble vibrations. The coupling of the TFV along with the motion of the hub induces a considerable aligning moment about the king-pin axis which in turns excites a toe

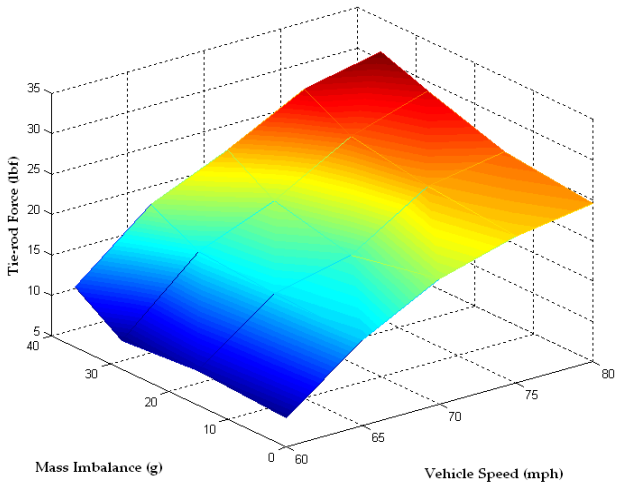

Figure 11. RMS tie rod forces vs. imbalance mass and speed

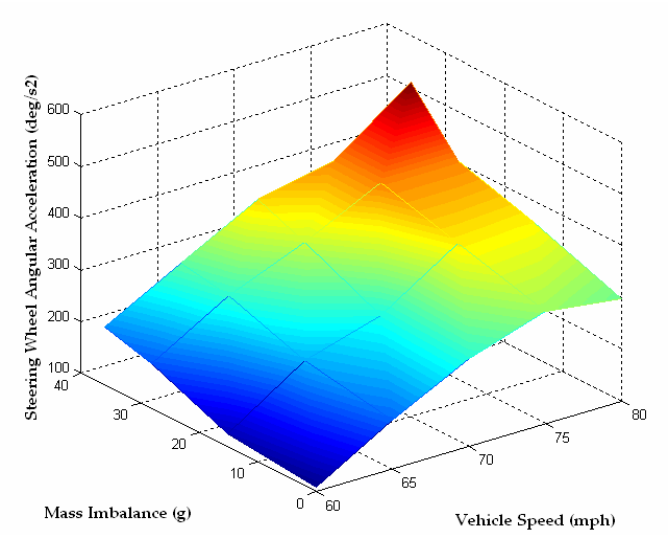

Figure 12. RMS steering wheel angular acc. versus imbalance mass and speed

mode of the suspension and thus generates a large force in the tie rod. The second harmonics induced by tire non-uniformity might also contribute to the generation of vibrations. However, they are significantly (almost an order of magnitude) lower than the first harmonic of the tire forces.

It is recommended to conduct a more extensive study of the nonlinear resonant frequency present in the steering system. This could be achieved by performing many more modal analysis tests to obtain a lot of information about the shift in the resonant frequency. Similarly, one could devise an optimization of the steering parameters (using least square methods or genetic algorithm for instance). The model presented herein does not consider the full vehicle dynamics. The development of a chassis model could be included to the present model to investigate the effect of chassis flexibility,

particularly the lateral bending and torsional bending modes. Once the new model is finely tuned, a larger sensitivity study could be conducted to investigate the effects of tire, suspension and chassis parameters.

Acknowledgement

The authors would like to express their appreciation for technical guidance and useful inputs to Mr. Julien Flament and Mr. Britton Martin of Michelin Americas R&D. The authors gratefully acknowledge and thank Michelin Americas R&D for the sponsorship and support of this research.

REFERENCES

[1] Attia, H.A., "Dynamic modeling of the double wishbone motor-vehicle suspension system", *European Journal of Mechanics and Solids*, **21**, pp. 167-174, 2002.

[2] Attia, H.A., "Numerical kinematic analysis of the double wishbone motor-vehicle suspension system", *Transactions of the Canadian Society of Mechanical Engineers*, **24**, pp. 391-399, 2000.

[3] Bosworth, R., "Application of taguchi method to solving steering wheel vibration", *Proceedings of the Institution of Mechanical Engineers*, pp. 347-360, 1989.

[4] Cherian, V., Jalili, N., Haque, I., "Development of a nonlinear model of a double wishbone suspension", *Proceedings of the ASME-International Mechanical Engineering Congress and Exposition*, Anaheim, CA, November 2004.

[5] Cherian, V., Jalili, N. and Virgile, A., "Tire nonuniformity induced tangential steering wheel vibrations: Part II - Experimental testing and validation", submitted to *Vehicle System Dynamics*, May 2005

[6] Demers, M., "Suspension bushing effects on steering wheel nibble", *Society of Automotive Engineers*, SAE 2003-01-1712, 2003.

[7] Dillinger, B., Jalili, N., Haque, I., "Analytical Modeling and Experimental Verification of Tire Non-uniformity", *International Journal of Vehicle Design*, in print, pp 1-22, 2006.

[8] Kim, J. W., Jeong S. K. and Yoo, W., "Sensitivity Analysis of Chassis System to Improve Shimmy and Brake Judder Vibration on Steering Wheel", SAE-960734, 1996.

[9] Kimura, T., Yoshifumi, H., Hiroshi, T., Fujisawa, K.., "Analysis of steering shimmy accompanied by sprung mass vibration on light duty truck – Fundamental mechanism", *JSAE Review*, **17** (3), pp. 301-306, 1996.

[10] Mancosu, F., Matrascia, G., and Cheli, F., "Techniques for Determining the Parameters of a Two-Dimensional Tire Model for the Study of Ride Comfort," *Tire Science and Technology, TSTCA*, **25**, pp. 187-213, 1997.

[11] Mangun, D., "Simulation of tire non-uniformity induced nibble vibrations through integrated subsystem modeling", *Master's Thesis*, Clemson University, December 2006.

[12] Morman, K.N., "Nonlinear model formulation for the static and dynamic analyses of front suspensions", *Society of Automotive Engineers*, SAE 770052, 1977.

[13] Neureder, U., "Modeling and simulation of the steering system for the investigation of steering nibble", *Automobil-technische Zeitschrift*, **103** (3), pp. 216-224, 2001.

[14] Neureder, U., "Investigation into steering wheel nibble", *Proceedings of the Institution of Mechanical Engineers, Part D: Journal of Automobile Engineering*, **216** (4), pp. 267-277, 2002.

[15] Pak, C. H., Lee, U., Hong, S. C., Song, S. K., Kim, J. H., Kim, K. S., "Study on the tangential vibration of the steering wheel of passenger car", *Proceedings of the 6th International Pacific Conference on Automotive Engineering*, pp. 961-968, Seoul, Korea, October 1991.

[16] Song, S.K., Pak, C.H., Hong, S.C., Oh, J.W., Kim, J.H., and Kim, S.C., "Vibration analysis of the steering wheel of a passenger car due to the tire nonuniformity", *Society of Automotive Engineers*, SAE 931918, 1993.

[17] Stutts, D. S., Soedel, W., Jha, S. K., "Fore-aft Forces in Tire-Wheel Assemblies Generated by Unbalances and the Influence of Balancing," *Tire Science and Technology, TSTCA*, **19**, pp. 142-162, 1991

[18] Takegawa T., Ohhara T., and Wakabayashi Y., "Brake Judder and Shimmy Simulation Technology Development", ESTECH Corp., *Customer Publication 41*, 2001, http://www.estech.co.jp/list.pdf/%20customer/cust41.pdf.

[19] Wang, D., and Rui, Y., "The Effects of front suspension parameters on road wheel toe dynamics", *Society of Automotive Engineers*, SAE 2001-01-0482, 2001.

APPENDIX A: NOMENCLATURE

Inertia of steering wheel, I_{hw} (kg-m^2)

Steering wheel angular displacement, θ_{sw} (radians)

Inertia of pinion, I_p (kg-m^2)

Pinion angular displacement, θ_p (radians)

Stiffness of torsion bar, K_{tbar} (N-m/rad)

Damping in torsion bar, C_{tbar} (N-m/rad/s)

Linear displacement of the rack housing, y (m)

Mass of rack housing, M_h (Kg)

Linear displacement of the rack, x (m)

Mass of rack, M_r (Kg)

Frictional compliance stiffness between the rack/rack housing interface, K_c (N/m)

Frictional compliance stiffness between the steering shaft and the chassis, K_{c2} (N-m/rad)

Compliant steering column friction, f_{sc} (N-m)

Compliant rack friction, f_r (N)

Hydraulic power assist boost rate, B (N-m/rad)

Damping due to hydraulic fluid, C_d (N/m/s)

Bushing stiffness of bushing connecting rack housing to chassis, K_h (N/m)

Damping in bushing connecting rack housing to chassis, C_h (N/m/s)

Angular Velocity of Coordinates $x_T y_T z_T$, $\boldsymbol{\Omega}$ (rad/sec)

Average Angular Velocity of Tread Ring, Ω_0 (rad/sec)

Tangential Displacement of Tread Ring Center of Mass, u_x (m)

Radial Displacement of Tread Ring Center of Mass, u_y (m)

Effective Rolling Radius of Rigid Tread Ring, R (mm)

Angular Displacement of Tread Ring, ϕ_T (rad)

Angular Displacement of Hub/Wheel, ϕ_H (rad)

Angular Location on Tread Ring, θ (rad)

Mass of Lumped Mass Imbalance, m_w (kg)

Location of Mass Imbalance on Tread Ring, θ_M (rad)

Tread Stiffness, k_T (N/m)

Mass of Tread Ring, M_T (kg)